Modeling and Simulation of WLAN Modem- Timing Recovery and Channel Estimation

Ming Ding and Zukang Shen

EE381K-11 Wireless Communications

Course Project Final Report

Supervisor: Prof. Robert W. Heath Jr.

{ming,shen}@ece.utexas.edu

May 3rd, 2002

Table of Contents

Abstract

Wireless Local Area Networks (WLANs) are gaining more and more attentions these days. The IEEE 802.11a standard specifies the next generation of high speed WLANs, which operate at UNII 5GHz band and provide bit rates from 6 Mbits/s to 54 Mbits/s in a 20 MHz bandwidth. In this project, We model a baseband OFDM transceiver for WLAN compatible with the IEEE 802.11a physical layer. Special attention has been paid to the receiver initialization. For optimal performance the receiver and transmitter must adapt to the channel and noise characteristics during initialization. The receiver must estimate the channel and noise, perform channel equalization and also synchronize to the transmitter. Zukang is more on timing recovery issue and Ming takes care of channel identification.

Chapter 1

Introduction

The Wireless Local Area Networks (WLANs) market is bloomed due to the need for a broadband high-speed wireless access technique. WLAN has several advantages over its wired counterpart, such as mobility, easy installation, reduced cost, and scalability. Different transmission technologies are adopted by different WLAN standards. For example, IEEE 802.11b uses direct sequence spread spectrum (DSSS) technique, Bluetooth uses frequency hopping spread spectrum (FHDS) solution, and IEEE 802.11a adopts ODFM scheme. WLAN can be used in various scenarios. University students can access professors' on-line notes in class. Doctors can get patients' record instantly. Passengers in airports can surf the Internet while waiting for a departure. All these exciting things are made possible by WLANs. Among all the WLAN standards, IEEE 802.11a is gaining more and more attention. This standard specifies an OFDM system, which works at UNII 5 GHz band. The system can provide bit rates from 6 Mbits/s to 54 Mbits/s in a 20 MHz bandwidth. This is the system we looked into this semester.

1.1 Overview of WLAN Modem

In transmission mode, payload data enters the symbol mapper where bits are mapped onto either BPSK, QPSK, 16-QAM or 64-QAM. The mapper provides a sequential series of 64 frequency domain samples to IFFT. The IFFT transforms the frequency domain constellation into a time domain sequence. Then cyclic prefix (CP) is added. The properly extended output of IFFT is denoted as an OFDM symbol. At last transmitted data sequence is sent to the low-IF upconversion stage [1].

In reception mode, data is provided from low-IF down-conversion stage to gain control and timing synchronization stage. The preambles serve to estimate gain, frame start and carrier frequency offset. The CP is stripped off before entering a FFT block. FFT translates received time domain samples into frequency domain. Equalizer performs an initial channel estimate, based on BPSK reference symbol in preambles. During data transmission stage, it divides the received constellation by its channel response per subcarrier and provides decision through the demapper [1].

1.2 Objectives

In this project, We modeled a baseband OFDM transceiver for high speed WLAN compatible with the IEEE 802.11a physical layer. Channel estimation and synchronization are the two specific issues we dealt with. We evaluated several ways to do channel estimation and synchronization. We also modeled a frequency selective fading channel, and the relative accuracy of the channel model is examined.

In this report, we give problem statement in Chapter 2. In Chapter 3, we explain how to build up our test platform for WLAN modem in MATLAB. We address the synchronization issue and channel estimation in Chapter 4 and 5 respectively. The conclusions are drawn in Chapter 6.

Chapter 2

Problem Statement

The IEEE 802.11a standard specifies OFDM as the modulation scheme. OFDM is becoming increasingly popular for high-speed wireless communications because of its strong immunity to multipath channels. The key point of an OFDM system is that cyclic prefix or guard interval is added to each OFDM symbol. As long as the multipath delay is shorter than the length of the cyclic prefix, an ISI free region can be found in each symbol. However, if the channel length is larger than that of the cyclic prefix, then time domain equalizer (TEQ) is needed to shorten the channel response. In WLAN scenario, the maximum excess delay is not long enough to pollute all the cyclic prefix samples. So there could be more than one valid window in an OFDM symbol and no TEQ is required. For coherent detection, we must estimate the channel and undo the channel distortion to get the transmitted information bits back. In OFDM system, channel equalization usually done in frequency domain after we estimate the channel transfer function. Synchronization is another important factor that can influence the system's overall performance much. Due to the high carrier frequency used in 802.11a standard, a small carrier frequency offset can introduce significant errors. In some cases, the samples can rotate 90 degree in a single OFDM symbol. Sampling clock error also degrades the performance by introduce inter sample interference.

Chapter 3

Test platform for WLAN modem

3.1 System build-up

We implemented a simple baseband WLAN system shown in Fig. 3.1. We have a 1/2 convolutional encoder, two-permutation interleaver, 16-QAM mapper, and 64-FFT blocks, as specified by the standards.

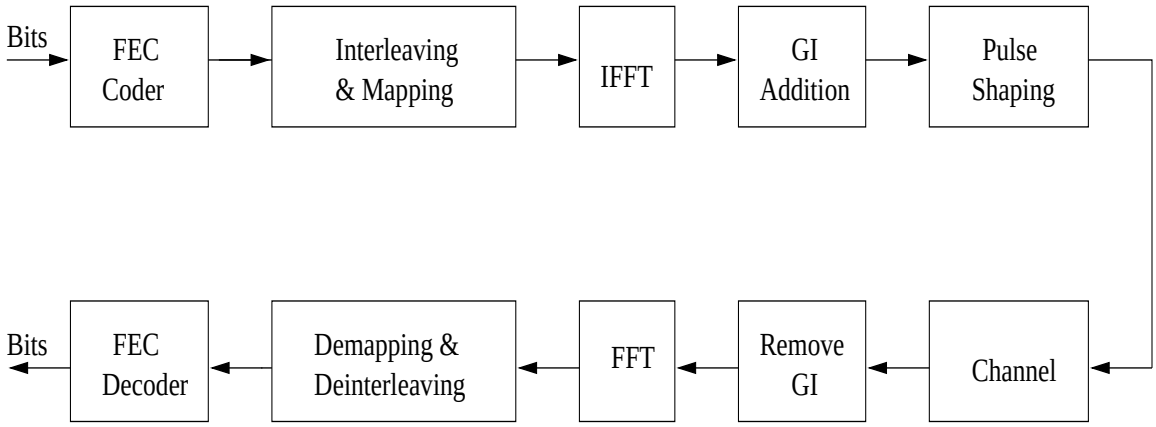

Figure 3.1: OFDM system basic block diagram

10 repetitions of short preambles and 2 repetitions of long preambles appear at the beginning of each OFDM frame. These preambles are used to carry out channel estimation and frequency offset estimation. Following the preambles is the SIGNAL symbol, which indicates the data rate and the length of this frame. Afterward is the payload data, with cyclic prefix properly extended. The baseband samples at the transmitter end can be

expressed as:

$$S(n) = \frac{1}{\sqrt{N}} \sum_{k=0}^{N-1} C_k e^{-j2\pi kn/N} \tag{3.1}$$

where $-L < n < N-1$. L is the cyclic prefix length and N is FFT size. C_k's represent the frequency domain data in an OFDM symbol. $S(n)$ is the time domain sample.

3.2 Channel Model

Clarke developed a model where the statistical characteristics of the electromagnetic fields of the received signal at the mobile are deduced from scattering. The model assumes a fixed transmitter with a vertically polarized antenna. The field incident on the mobile antenna is assumed to be comprised of N azimuthal plane waves with arbitrary carrier phase, arbitrary azimuthal angles of arrival, and each wave having equal average amplitude. The vertical E field can be expressed as:

$$E_z = T_c(t)\cos(2\pi f_c t) - T_s(t)\sin(2\pi f_c t) \tag{3.2}$$

where:

$$T_c(t) = E_0 \sum_{n=1}^{N} c_n \cos(2\pi f_n(t) + \phi_n) \tag{3.3}$$

$$T_s(t) = E_0 \sum_{n=1}^{N} c_n \sin(2\pi f_n(t) + \phi_n) \tag{3.4}$$

where c_n, f_n and ϕ_n are the amplitude of the nth incident wave, the Doppler frequency shift of the nth incident wave, and the initial phase for the nth incident wave, respectively. And it can be shown that the envelop of E_z has a Rayleigh distribution as N is sufficiently large. Since we want to simulate a frequency selective channel and Clarke's model only provides a way for flat fading channel modeling, we built up several independent Rayleigh

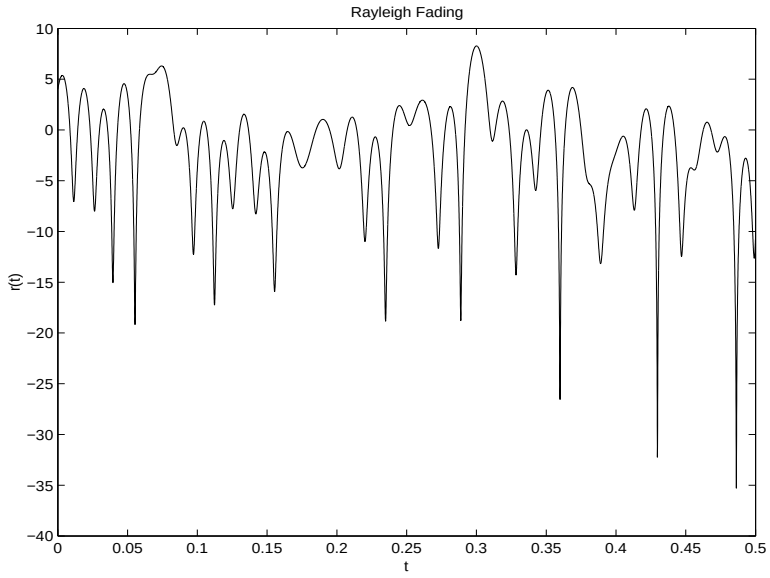

Figure 3.2: Rayleigh Fading

fading channels to simulate different multipaths. And the exponential power delay profile model is used to scale the relative power of each multipath.

Since the maximum excess delay of indoor environment is around 300 ns and the sampling clock period of the system is 50 ns, we modeled the frequency selective channel as a 6-tap FIR filter. Six independent Clarke's models were used to simulate the frequency selective channel. Fig. 3.2 plots the envelope of one Clarke's model and fig. 3.3 compares the simulated channel's auto-correlation function with the theoretical function, which is the zero order, first kind Bessel function.

From Fig. 3.3, we can see that the simulated channel's auto-correlation function matches well with the ideal one at the beginning, but deviates from the theoretical one when the time separation increases. Other simulation methods, such as Jakes' method, can provide channel models which have more precise auto-correlation functions. The reason we simulated the channel directly from Clarke's model is that we have to generate six Rayleigh flat fading channels to model different multipaths, and we want them to be as lit-

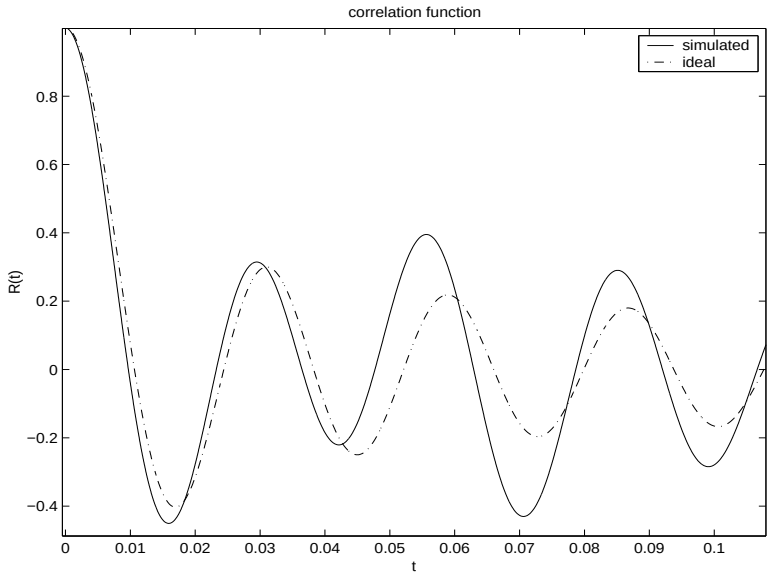

Figure 3.3: Autocorrelation Function

tle dependent on each other as possible. If Jakes' method is adopted, the cross-correlation between different multipath channels would be relatively large.

Chapter 4

Synchronization

4.1 Frequency offset and Timing error

Besides the channel distortions applied to OFDM symbols, carrier frequency offset and sample clock error can also degrade the performance. The carrier frequency offset is caused by the frequency difference between the local oscillators at the transmitter and receiver respectively. It can be modeled by multiplying the received time domain signal by a complex exponential:

$$r(n) = e^{j2\pi f_e n T_s} s(n) * h(n) \tag{4.1}$$

where f_e is the carrier frequency offset, $s(n)$ is the transmitted time domain sample and $h(n)$ is the channel impulse response. Note that both $s(n)$ and $h(n)$ are complex values. The sampling clock error can be modeled by time domain interpolation. We use a raised cosine ($\alpha = 1/2$) function as our pulse-shaping filter. The filter is truncated from -$3T_s$ to $3T_s$. One straightforward way to introduce the sampling clock error is to over-sampling the signal by a factor of M. The received signal can be expressed as:

$$r(n,m) = r((n + m/M)T_s) = e^{j2\pi f_e n T_s} s(n) * h(n) * g(n,m) \tag{4.2}$$

where

$$g(n,m) = \frac{\sin(\pi(n + m/M))}{\pi(n + m/M)} \frac{\cos(\pi(n + m/M)\alpha}{1 - (4\alpha(n + m/M)/2)^2} \tag{4.3}$$

where $n = -3, -2, -1, 1, 2$ and $m = 0, 1, 2, \ldots, M$.

From the over-sampled signal $r(n,m)$, we can choose whatever sampling clock error value (with a resolution of 1/M T_s) as we want. However, we can see a huge waste of

computations since we only need one output sample every M interpolated values. The solution to this problem is to find a correct $g(n, m)$ for each input $s(n)*h(n)$. For example, if the sampling clock period is $(1 + k/M)T_s$, and assuming at time n_0, there is a perfect alignment, then $r(n)$ can be expressed as:

$$r(n) = e^{j2\pi f_e n T_s} s(n) * h(n) * g(n, \mathrm{mod}((n - n_0)k, M)) \tag{4.4}$$

4.2 Synchronization

Various schemes are proposed to deal with frequency offset and timing errors. [2] presents a maximum likelihood estimator of carrier frequency offset for multicarrier signals in frequency selective Rayleigh fading channels. [3] proposed a pilot-based method to perform timing recovery in OFDM systems. We use a very simple but effective way to do the synchronization. This method is proposed by Karthik Ramasubramanian and Kevin Baun in [4]. For the received signal r(n), a correlation value is calculated by the following equation:

$$\rho(n) = \frac{\left|\sum_{m=0}^{M-1} r^*(n + m(N + L))r(n + m(N + L) + N)\right|}{\sqrt{\sum_{m=0}^{M-1} |r(n + m(N + L))|^2}\sqrt{\sum_{m=0}^{M-1} |r(n + m(N + L) + N)|^2}} \tag{4.5}$$

where N is the FFT size and L is the cyclic prefix length. This method tries to multiply the sample in the cyclic prefix with an identical sample, which is N samples later, in the same OFDM symbol. And correlation is evaluated over M OFDM symbols to increase the accuracy. An appropriate threshold is chosen to indicate an ISI free region. This method has an advantage that the delay spread caused by the channel can be estimated. Assuming the length of the cyclic prefix is L, and the length of the detected ISI free region is I, it is obvious that the channel spread is L-I+1. However, the disadvantage of this method is that the correlation is done over many OFDM symbols, which leads to either large delays or high memory requirements in implementation.

Fig. 4.1 shows the simulation results. In the simulation, we introduced a sampling clock offset of 20 ppm by using the interpolation method discussed previously. The correlation

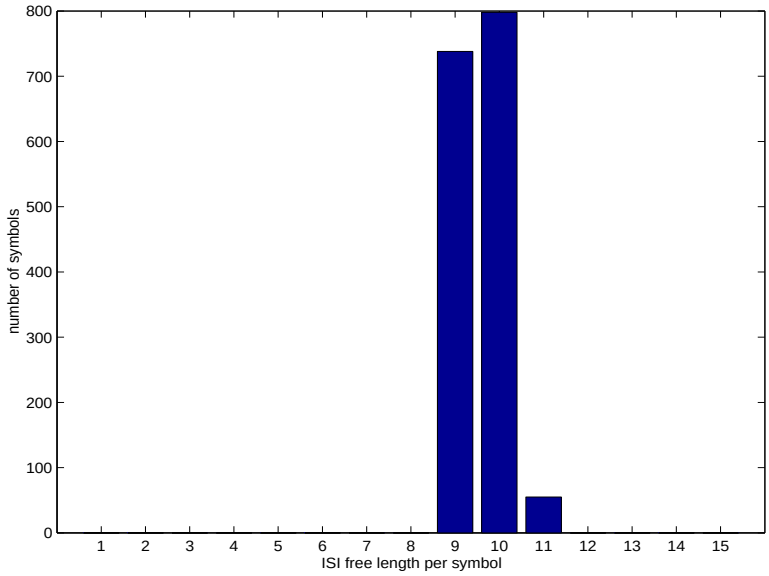

Figure 4.1: ISI free length

value is done over 200 OFDM symbols. And the threshold value is chosen to be 0.9999. Since the channel model is a 6-tap FIR filter and the cyclic prefix length is 15 (the cyclic prefix length is not 16 because the first sample in an OFDM symbol is overlapped with the last sample of the previous symbol), the accurate length of ISI free region in an OFDM symbol is 10. From Fig. 4.1, we can see that in almost half of the OFDM symbols, the whole ISI free region is recovered, while in nearly another half, the detected region is a little tight, due to the high threshold value we choose. Actually, the threshold value means a lot to the performance of the method proposed in [4]. The detected ISI free region will be tight or loose, depending on the value of the threshold, which is closely related to the average error in the system, such as frequency errors, timing error and additive white Gaussian noise. And we prefer tight regions instead of loose regions. So the threshold should be a little high at the beginning. [4] did not provide a way to do frequency offset and timing error correction. [5] proposed a way to correct both the carrier frequency offset and the timing error. We can expect that when the errors are somewhat corrected, the

correlation threshold value should be adaptively changed in order to estimate the whole ISI free region more accurately. This could be the future work.

Chapter 5

Channel Estimation

Coherent OFDM detection requires channel estimation and tracking. In an IEEE 802.11a packet, long preambles carry BPSK modulated signals on 52 subcarriers, which can be used for channel estimation. Typical channel estimation is either performed in time domain to measure the impulse response or carried out in frequency domain to estimate the channel transfer function for specified frequencies.

5.1 Characterizing the WLAN channel

Some wireless OFDM systems, such as Digital Video Broadcasting (DVB) or Digital Audio Broadcasting (DAB), require special channel estimation schemes for frequency-selective time-variant channels. These schemes have to estimate the time variance of the channel as well as the frequency selectivity. Furthermore, in mobile OFDM systems, large Doppler frequency shift results in an error floor due to intercarrier interference (ICI). Pilot based channel estimation schemes have to cope with it, since pilots will be ICI corrupted too. However, IEEE 802.11a is mostly a wireless digital communication system in indoor environments. The indoor channel can be considered quasi-static due to limited object movements [1]. The coherence time is on the order of tens of milliseconds, while the duration of a cyclic-extend OFDM symbol is 4 microseconds. Thus, time interpolation of the channel estimates between pilot symbols is not needed. Surely we should estimate the channel at least every coherence time duration. On the other hand, the in-house channel is characterized by a rms delay spread of 40 to 500 ns. The coherence bandwidth is between 0.4 to 5 MHz which, compared to the 20 MHz channel bandwidth, reveals the

frequency selective nature of the indoor channel. Also, preamble contains pilots for each subcarrier. This enables us to estimate transfer function at the bands of interest without interpolation in the frequency domain.

5.2 Estimation of Channel Impulse Response (CIR)

There are several pilot-aided channel impulse response estimation schemes for OFDM systems available. The maximum likelihood estimator (MLE) and the Bayesian minimum mean square error estimator (MMSEE) are two popular approaches among them. MLE treats CIR as a deterministic but unknown vector while MMSEE looks CIR as a random vector whose practical instantiation we want to estimate [6].

Typical OFDM system exploits IDFT-DFT to transform avaliable bandwidth into a set of orthogonal and equally-spaced subbands. The information data is encoded in frequency domain before IDFT at the transmitter and must be recovered after DFT at the receiver. Usually a total of N_p pilots $\{a_n; 0 \leq n \leq N_p - 1\}$ are put in the tones $\{i_n; 0 \leq n \leq N_p - 1\}$. The DFT output at the pilot tones could be written as $\mathbf{X} = [X(i_0), X(i_1), \ldots, X(i_{N_p})]^T$. We form $\mathbf{Z} = \mathbf{A}^H \mathbf{X}$, where $\mathbf{A}$ is a diagonal matrix: $\mathbf{A} = \text{diag}\{a_0, a_1, \ldots, a_{N_p}\}$. Then

$$\mathbf{Z} = \mathbf{B}\mathbf{h} + \tilde{\mathbf{w}}$$

holds, where $\mathbf{B}$ denotes the DFT matrix, $\mathbf{h}$ is the CIR vector and $\tilde{\mathbf{w}}$ is the additive noise vector.

The estimate of $\mathbf{h}$ under MLE is given by

$$\hat{\mathbf{h}}_{MLE} = (\mathbf{B^H B})^{-1} \mathbf{B}^H \mathbf{Z},$$

with the mean square error (MSE) is the average over the observed data. On the other hand, the estimate of $\mathbf{h}$ under MMSEE is found to be

$$\hat{\mathbf{h}}_{MMSEE} = (\sigma^2 {\mathbf{C_h}}^{-1} + \mathbf{B^H B})^{-1} \mathbf{B}^H \mathbf{Z}$$

where $\mathbf{C_h}$ is the covariance matrix of $\mathbf{h}$. MLE could achieve the Cramér-Rao lower bound (CRLB), which is the minimum-variance unbiased estimator. MMSEE adopts a Bayesian MSE approach to outperform (CRLB) provided the sufficient prior information is available, such as channel covariance and noise variance.

The main advantage of MLE over MMSEE is that it does not require knowledge of the channel statistics and the SNR. Therefore, it is simpler to implement. Under certain operation conditions, the MMSEE has better accuracy as it exploits prior information about the channel. It is reported that the two schemes have comparable performance at intermediate and high SNRs as long as the number of pilots is larger than the taps of CIR. We only simulated MLE in this project. The performance is not so good as the transfer function measuring schemes in terms of mean square error at the output of FFT.

5.3 Estimation of Channel Transfer Function

In the transmitter, the main functions are convolutional coding, bit interleaving, modulation and IFFT. In the receiver, assuming perfect synchronization, the 1-tap channel estimator/equalizer banks are implemented after FFT. The channel effect on each subcarrier after FFT is a complex coefficient on the condition that the ICI is very small and could be ignored. We mainly studied several algorithms based on minimum mean square error (MMSE) criterion, which minimize the MSE between the transmitted symbol and its estimate.

5.3.1 A deterministic identification scheme

The scheme we adopted is developed by [7], which is basically a nonparametric approach where a direct estimation of the system frequency response is made. Very narrow band filters centered at various frequencies (DFT filter banks in our case) are used to extract the

magnitude and phase of the input and output signals at a set of pre-specified frequencies. The frequency response of the system at each of these frequencies is the ratio of the output signal to the corresponding input signal. A least-squares optimization process is used in the frequency domain to obtain the enough samples of the transfer function. Then the time domain samples of impulse response of the channel can be easily obtained by applying an inverse discrete Fourier transform (IDFT).

Generally, the values of the transfer function of the channel at various frequency points can be computed by

$$W_i = P(e^{j2\pi i/N}) = \frac{Y_i}{U_i}, \quad i = 0, 1, ..., N-1 \tag{5.1}$$

where U_i are the DFT samples of one period of plant input u_k and Y_i are the DFT samples of the corresponding cycle of y_k. Using least-squares optimization techniques to minimize

$$\xi_i = \sum_k |Y_{ik} - W_i U_{ik}|^2. \quad i = 0, 1, \ldots, \frac{N}{2}, \tag{5.2}$$

we obtain

$$W_i = \frac{\sum_k Y_{ik} U_{ik}^*}{\sum_k |U_{ik}|^2}, \quad i = 0, 1, \ldots, \frac{N}{2}. \tag{5.3}$$

We only consider the samples we obtained after the transient time, i.e., $k > L + N$ where L indicates the transient times. We note u_k is periodic with period N, U_{ik} is also periodic in k with period N. If we select samples with the spacing of N, U_{ik} will be constant. If the time index of the first considered sample is k_0 and totally N_s samples are selected, the transfer function can be simply computed by

$$W_i = \frac{1}{N_s U_{ik_0}} \sum_{l=0}^{N_s-1} Y_{i(k_0+lN)}, \quad i = 0, 1, \ldots, ..., \frac{N}{2}. \tag{5.4}$$

Interchanging the summation and DFT, we can get the input to DFT as

$$y_i' = \sum_{l=0}^{N_s-1} y_{k_0+lN-i}. \quad i = 0, 1, \ldots, N-1 \tag{5.5}$$

The sample U_{ik_0} maybe read from a look-up table.

This method could be easily applied to our case, where U_i is the pilot for ith subband. Simulation of this method shows the mean square error is on the order of 10^{-3} for average on 50 symbols.

5.3.2 Least-mean squares (LMS) method

The LMS algorithm is the basic adaptive algorithm for implementing MMSE optimum estimator. Due to the complex nature of the tap coefficients, the complex LMS is adopted here to update the taps:

$$\begin{aligned} err_I &= Y_I - (\hat{H}_I * P_I - \hat{H}_Q * P_Q) \\ err_Q &= Y_Q - (\hat{H}_I * P_Q + \hat{H}_Q * P_I) \\ \hat{H}_I &= \hat{H}_I + \mu * (err_I * P_I - err_Q * P_Q) \\ \hat{H}_Q &= \hat{H}_Q + \mu * (err_I * P_Q + err_Q * P_I) \end{aligned} \tag{5.6}$$

where err, μ, Y, $\hat{H}$ and P are estimation error, step size, FFT output, estimated transfer function and pilots, respectively. The subscript I means real part and Q means imaginary part.

The learning curve is plotted in Fig. 5.1. The estimation error here is supposed to be norm of the 2 dimensional error signal. The step size is chosen to be 0.01. Slow Rayleigh fading channel with AWGN is assumed.

5.3.3 Recursive Least Squares (RLS) Method

For the RLS algorithm, we have the following equations to update for the estimator tap:

$$\hat{H}_{p+1} = \hat{H}_p + K_p(Y_p - \tilde{Y}_p) \tag{5.7}$$

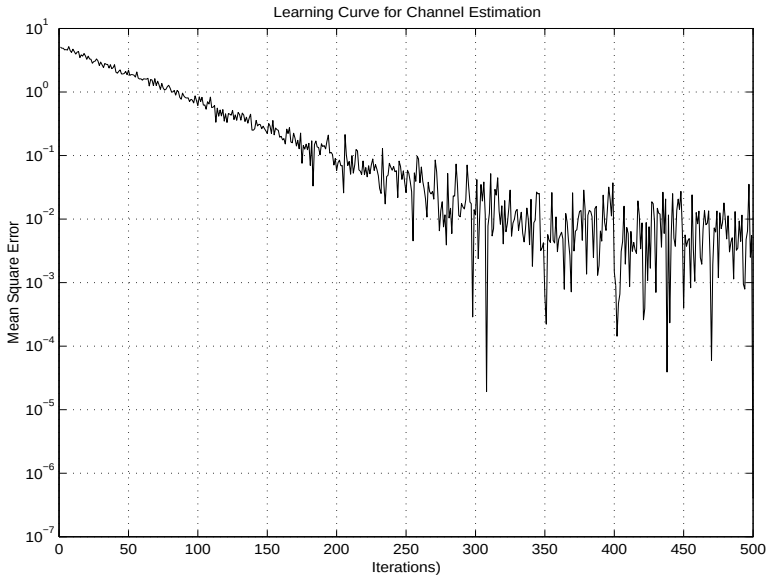

Figure 5.1: Learning Curve for LMS channel estimation

where Y_p is the FFT output, $\tilde{Y}_p$ is the decision made on the output and K_p is the Kalman gain. The forgetting factor in the simulation is chosen to be $\lambda = 0.9$ and initial matrix $\Psi_\lambda^{-1} = 1/(0.01)\mathbf{I_N}$, where $\mathbf{I_N}$ is $N \times N$ identity matrix. The details of standard RLS algorithm can be found in most of the adaptive signal processing books.

The learning curve of RLS algorithm is plotted in Fig. 5.2 The same transmission environment configuration is used as the LMS simulation. From the figure, we found the convergence speed of RLS is much faster than that of LMS, which makes RLS a favorable choice of real time implementation.

5.4 Common Phase Error Detection

The common phase error (CPE) results from imperfections of the oscillators used for modulation and demodulation. Though they are supposed to provide a stable frequency, real oscillators tend to provide a frequency that is slowly varying in time. This change in time leads to an additional modulation on the OFDM symbols, which in some cases must

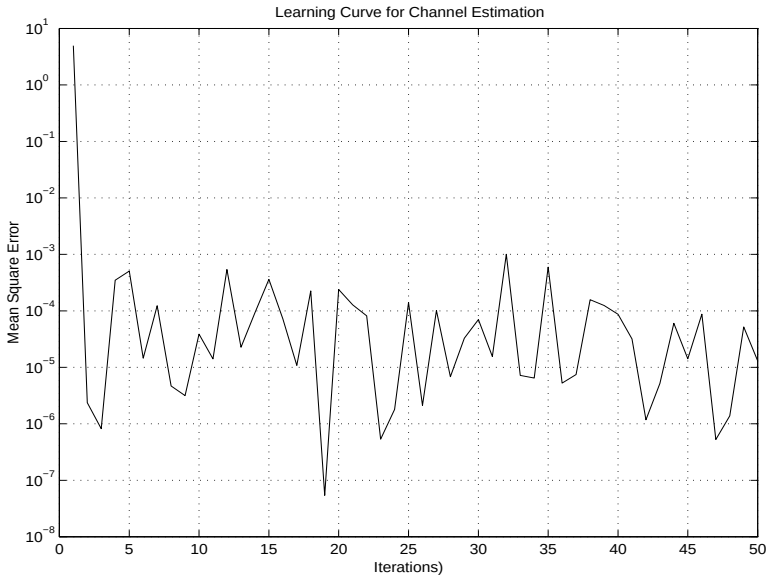

Figure 5.2: Learning Curve for RLS channel estimation

be estimated and compensated. Other sources of common phase error could be phase noise added in the down-converter by digital processing in the chip. Usually, The output data from the FFT is passed to the common-phase-error correction block. It is able to remove the common phase error because all subcarriers within a given symbol suffer the same common phase error. By measuring the continual pilots, the common phase error is determined and then subtracted from the phase of all the data cells in the same symbol [8].

Chapter 6

Conclusions

A test platform of OFDM based WLAN system is built up in MATLAB. All matlab codes are available on line. The frequency selective channel is well studied and modeled. A computational efficient way of introducing timing error is presented. We also evaluate the performance of several synchronization and channel estimation schemes. Recursive Least Squares method has been chosen for our receiver channel estimation and equalization. Simulation results show the OFDM receiver architecture is capable of high-rate data transmission in indoor multi-path fading channels. Future work could be optimal preamble design to achieve better performance in synchronization and channel estimation.

Bibliography

[1] Wolfgang Eberle, Veerle Derudder, Geert Vanwijnsberghe, Mario Vergara, Luc Deneire, Liesbet Van der Perre, Marc G.E.Engels, Ivo Bolsens and Hugo De Man, "80-Mb/s QPSK and 72-Mb/s 64-QAM Flexible and Scalable Digital OFDM Transceiver ASICs for Wireless Local Area Networks in the 5-GHz Band", *IEEE Journal of solid-state circuits*, vol. 36, no. 11, pp. 1829-1838, Nov. 2001.

[2] Yang-Seok Choi, Peter J. Voltz and Frank A. Cassara, "ML Estimation of Carrier Frequency Offset for Multicarrier Signals in Rayleigh Fading Channels", *IEEE Trans. on Vehicular Tech.*, vol 50, No 2, March 2001.

[3] Baoguo Yang, Khaled Ben Letaief, Roger S. Cheng, and Zhigang Cao, "Timing Recovery for OFDM Transmission", *IEEE Journal on Secelected Areas in Comm.*, vol 18, no 11, Nov. 2000.

[4] Karthik Ramasubramanian and Kevin Baum, "An OFDM Timing Recovery Scheme with Inherent Delay -Spread Estimation", *IEEE GLOBECOM '01*, vol 5, pp. 3111-3115, 2001.

[5] Rob Heaton, Steven Duncan, and Ben Hodson, "A Fine Frequency and Fine Sample Clock Estimation Technique for OFDM Systems", *IEEE Vehicular Technology Conference*, vol 1, pp. 678-682, 2001.

[6] Michele Morelli and Umberto mengali, "Comparison of Pilot-Aided Channel Estimation Methods for OFDM Systems", *IEEE trans on Signal Processing*, vol 49, no 12, pp. 3065-3073, Dec. 2001.

[7] B. Farhang-Boroujeny and Teng-Tiow Tay "Transfer Function Identification with Filtering Techniques," *IEEE Trans. on Signal Processing*, vol. 44, no 6, pp. 1334-1345, June 1996.

[8] Chien-Fang Hsu, Yuan-Hao Huang and Tzi-Dar Chiueh, "Design of an OFDM Receiver For High-speed Wireless Lan", *IEEE International Symposium on Circuits and Systems*, vol 4, pp. 558-561, 2001.